Egyptian Geophysical Society
EGS Journal, Vol. 13, No. 1, 127-140 (2015)

IDENTIFYING THE DUWI FORMATION IN ZOG EL-BOHAR AREA, CENTRAL EASTERN DESERT OF EGYPT USING GROUND GAMMA-RAY SPECTROMETRY

S.E. Abdelwahab[(1)], A. A. Nigm[(2)], A. Abdelgawad[(1)],
M.A. Gouda[(2)] and I.M. Khalil[(2)]

(1) Department of Geophysics, Faculty of Science, Ain Shams University.
(2) Nuclear Materials Authority (NMA), P. O. Box 530 El Maadi, Cairo, Egypt.

تعريف تكوين الضوى في منطقة زج البهار، صحراء مصر الشرقية،
بإستخدام الطرق الإشعاعية الأرضية

الخلاصة: إن تعريف وتحديد النطاقات الغنية بالتركيزات العالية للعناصر المشعة لمنطقة ما هو أحد التطبيقات الهامة للطرق الإشعاعية . أيضا إن طبقات االفوسفات الحاملة لليورانيوم الموجودة في تكوين الضووى هي من إحدى أهداف التنقيب عن اليورانيوم في صحراء مصر الشرقية والغربية . لهذا السبب استخلصت البيانات الطيفية لأشعة جاما الأرضية من منطقة زج البهار، وسط الصحراء الشرقية، مصر . بفحص البيانات المستخلصة من منطقة الدراسة تبين أنها سجلت ٥٢,٦ (يو.أر) لإجمالي العد الإشعاعي الكلي و ٥١ جزء في المليون من اليورانيوم المكافيء و ١٤ جزء في المليون من الثوريوم المكافيء و ٤,٢٪ من نسبة تركيز البوتاسيوم. وقد تم تحليل البيانات ومعالجتها باستخدام تقنيات تحليل فعالة مثل معامل التحليل و الصور المركبة الثلاثية وكذلك العديد من المعالجات الإحصائية. و قد أمكن تحديد خمس وحدات (ليثو–إشعاعية) في منطقة الدراسة من خلال القياسات الإشعاعية. هذه الوحدات (الليثو–إشعاعية) تتوافق بدرجة عالية مع الوحدات الليثولوجية السطحية للمنطقة . كما أظهر التحليل الإحصائي للبيانات المقاسة أن الفوسفات الحامل لليورانيوم الموجود في تركيب الضووى قد سجل أعلى القيم الإشعاعية في منطقة الدراسة. لذلك فإن النطاقات الغنية باليورانيوم في منطقة الدراسة تنسب لتكوين الضووي.

ABSTRACT: *Identifying and outlining zones of enriched radioelement concentrations of an area is among the applications of the radiometric methods. The uranium-bearing phosphate beds of the Duwi Formation are targets for uranium exploration in the Egyptian Eastern and Western deserts. For this purpose, the ground gamma-ray spectrometric data of Zog El-Bohar area, central Eastern desert of Egypt is utilized. Examination of the data in the area of study records 52.6 Ur for Total Count (TC), 51 ppm equivalent Uranium (eU), 14 ppm equivalent Thorium (eTh) and 4.2 % Potassium (K). The data were analyzed and processed using effective analysis techniques such as factor analysis, ternary composite imaging as well as the statistical treatments.*

Five litho-radiometric units could be delineated in the area from the radiometric point of view. These units are highly correlated with the surface geology of the area. Statistical analysis showed that the uranium-bearing phosphates Duwi Formation represents the highest radiometric values measured in the area. So, the Uranium-enriched provinces recorded in the area are mainly related to this formation.

INTRODUCTION

Previous geological, geophysical and geochemical studies proved that Zog El-Bohar area is charachterized by considerable extensions of the black shales (oil shales) of the Dakhla Formation in the subsurface. Oil shales can be used as source of petroleum, as fuel in thermal power plants and can be used for uranium and other rare chemical element production (Dyni, 2006 and USGS, 2007). In additions, the uranium-bearing phosphates of the Duwi Formation are highly exposed in the area. Due to the economical importance of oil shales in different industries as well as the importance of the phosphate of the Duwi Formation, the area of Zog El-Bohar attracts the attention of many workers. The area is located at about 15Km to southwest Quseir on the Red Sea Coast, Central Eastern Desert of Egypt between latitudes 25° 57′ 49.29″ N & 25° 58′ 27.91″ N and longitudes 34° 17′ 25.92″ E & 34° 18′ 11.31″ E (Fig. 1).

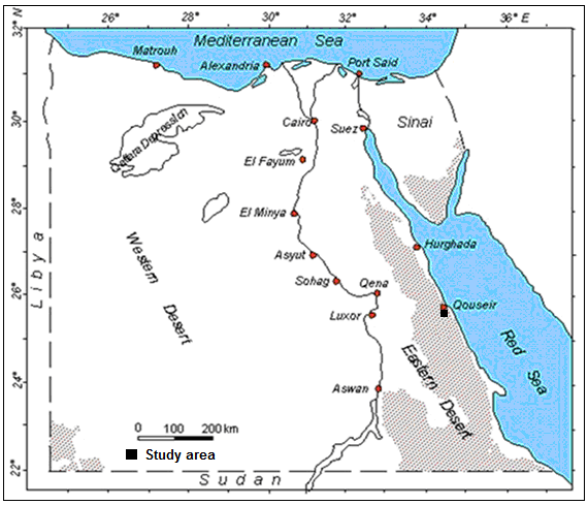

Fig. (1): Map of Egypt showing the location of Zog El=Bohar area.

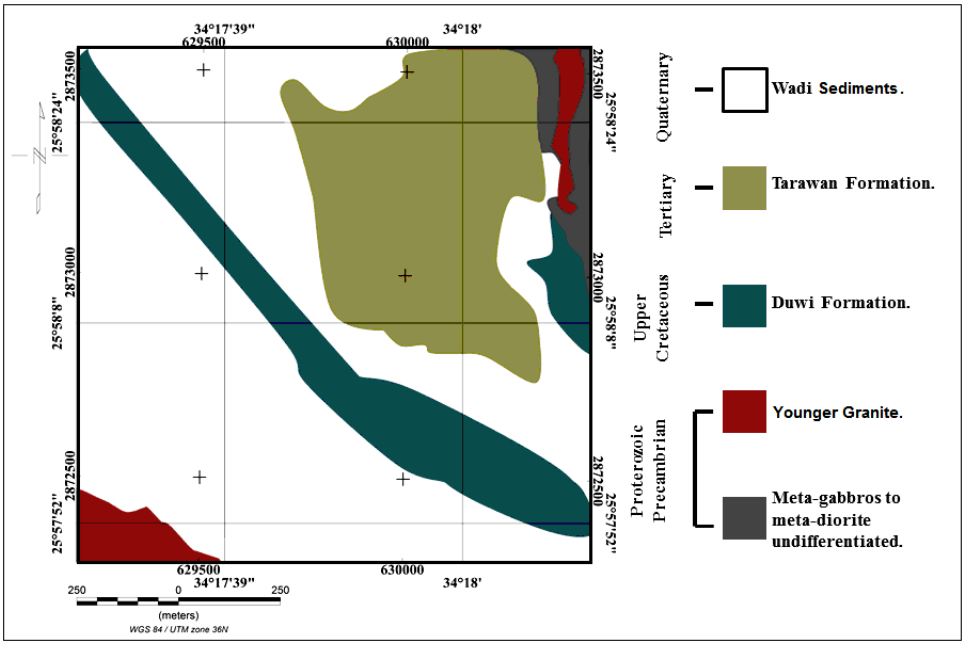

Fig. (2): Detailed simplified geologic map of Zog El-bohar area (after Sabet, 1976).

The ground spectrometric survey was carried out along 26 parallel profiles striking N-S, with line spacing 50m apart and station separation 25m along traverses. The collected data involve the total count (TC) in Ur, equivalent uranium (eU) in ppm, equivalent thorium (eTh) in ppm and potassium concentration (K) in %. A gamma-ray spectrometer, model GS-512, Czech made is used in the present survey.

GEOLOGIC SETTING

The geology of the area and its vicinity is described by many authors such as Barron and Hume (1902), Ball (1913), Beadnell (1924), Youssef (1957), Faris and Hassan (1959), Akkad and Dardir (1966), Abdel Razik (1967 and1972), Issawi et al., (1969 and 1971), Tarabili (1966 and 1969) and Gindy et al., (1973 and 1976) .Since the study area is relatively small, field observations proved its simple geologic setting where it consists of metagabbro, younger granite, Duwi Formation, Dakhla shales and Quaternary sediments. The Fig. (2) Depicted the simple geology of the area under consideration.

The Precambrian rocks in the area are represented mainly with the metagabbro and younger granites. The metagabbro is the oldest unit in the area and mainly recorded at the northeastern corner of the area. The ultramafic bodies consist mainly of serpentinite, associated with many lenses and pockets of chromite ores with different sizes, and less abundant talc carbonate rocks as well as minor amounts of ultramafic schists (Ahmed and Arai 2002). The younger granites have somewhat uniform composition, and consist principally of microcline, orthoclase, perthite, oligoclase, quartz, biotite, and/or hornblende. El Shazly and Abdallah (1964) and El Shazly (1977), considered the granites as late orogenic or third basement plutonite, that represent the last event in the evolution of the geosyncline in the Eastern Desert of Egypt.

Due to its uranium potentiality, the Duwi formation acquires special importance. It conformably overlies the Quseir variegated shale and underlies the Dakhla Shale. According to El Shazly (1977), the phosphatic offshore facies is one of the marine Late Cretaceous sediments in Egypt, occuring between 25° to 27° N. They extend from El Quseir-Safaga on the Red Sea to Qena- Idfu in the Nile Valley. He stated that the principal phosphatic facies are Campanian-Maestrichtian in age. This formation is a sequence of alternating beds of claystone, sandstone, calcareous mudstone, siltstone, siliceous mudstone bearing Ostrea Villei and oyster limestone enclosing a number of phosphate and phosphatic rock horizons. It exhibits features of depositions on an oscillating bottom of a shallow shelf and it is Late Cretaceous (Conoco, 1989).

A carbonate bed is easily recognized in Quseir area due to its sharp contact with the overlying and underlying dark green shales. This bed is equivalent to the Tarawan Chalk of Western Desert's oases. This formation is made up of marl and marly limestone. The Quaternary sediments bound the different rock units in the study area and fill the main wadies. These sediments include sands, pebbles and rare boulders mainly derived from meta-gabbros and granitic rocks as a result of the weathering and denudation processes for the surrounding hills and basement rocks.

The structural setting of the area under consideration is affected with the red sea rift system which exhibit superb outcrop examples of kilometric scale, extensional fault-related folds. The faults of the rift border fault system consist of series of WNW and NW-trending segments (Khalil and McClay, 2002).

DATA PROCESSING

The ground spectrometric survey of the study area provided information about the distribution and hence about the total-count of gamma radiation (TC) in Ur (Fig. 3) and the absolute concentrations of the three radioelements; equivalent uranium (eU) in ppm (Fig. 4), equivalent thorium (eTh) in ppm (Fig. 5) and potassium (K) in % (Fig. 6). In additions, three radioelements ratios eU/eTh (Fig. 7), eU/K (Fig. 8) and eTh/K (Fig. 9) were computed to visualize the relative concentrations of the radioactive-elements.

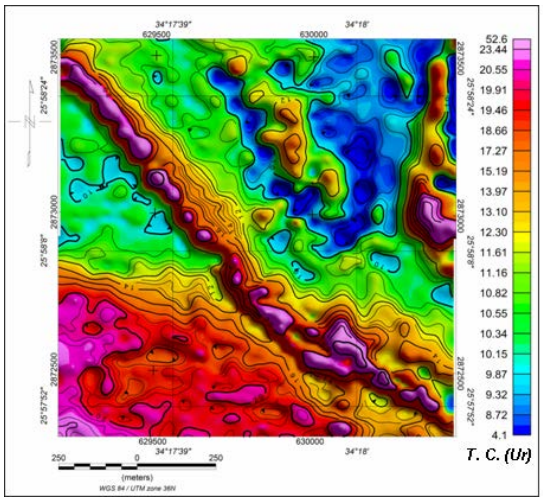

Fig. (3): Filled colored contour map of Total Count (TC) in Ur.

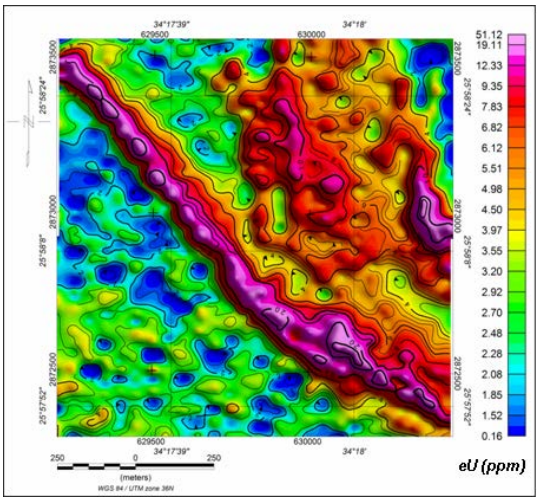

Fig. (4): Filled colored contour map of equivalent Uranium (eU) in ppm.

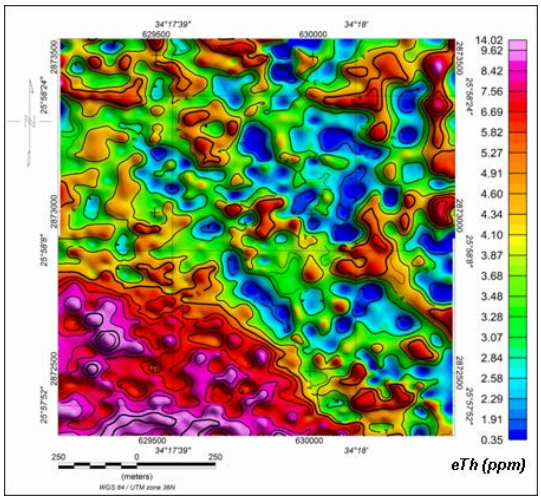

Fig. (5): Filled colored contour map of equivalent Thorium (eTh) in ppm.

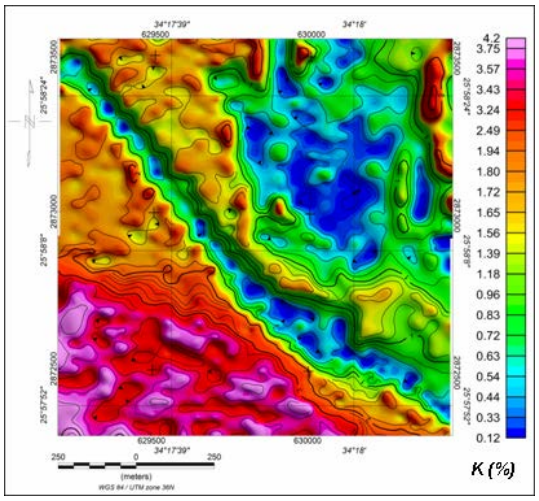

Fig. (6): Filled colored contour map of Potassium (K) in %.

color enhancement for the remaining data (IAEA,

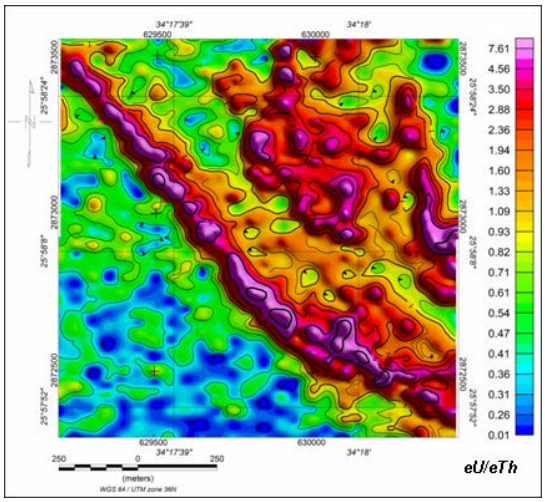

Fig. (7): Filled colored contour map of equivalents uranium/ thorium ratio (eU/eTh).

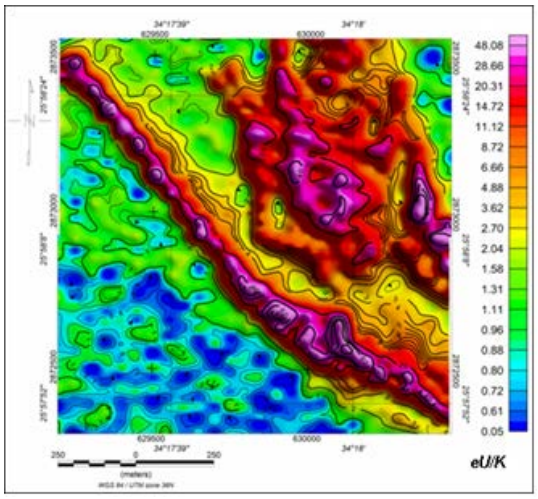

Fig. (8): Filled colored contour map of equivalent uranium/potassium ratio (eU/K).

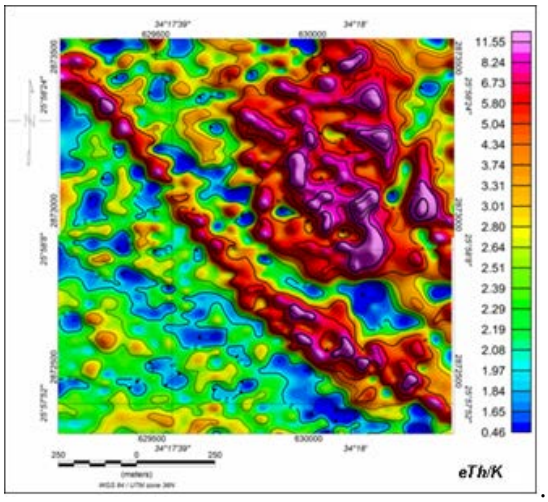

Fig. (9): Filled colored contour map of equivalent thorium/potassium ratio (eTh/K)

ANALYSIS TECHNIQUES

1. Composite Imaging

Composite color image, produced from gamma-ray spectrometric data, provide an interpretation with a useful synthesis of the data, which can be used as a tool for geological and geochemical mapping and mineral exploration (Duval 1983). A ternary radioelement map is a color composite image generated by modulating the red, green and blue phosphors of the display device or yellow, magenta and cyan dyes of a printer in proportion to the radioelement concentration values of the K, eTh, eU and TC grids. The use of red, green and blue for K, eTh and eU, respectively, is standard for displaying the gamma-ray spectrometric data. Blue is used to display the eU channel, since this is the noisiest channel and the human eye is least sensitive to variations in blue intensity. Areas of low radioactivity, and consequently low signal to noise ratio, can be masked by setting a threshold on the total count grid. These reserves more color space and ensures a better

2003).

Since particular rock types often have characteristic ratios of the three radioactive elements, the ternary map of these ratios is a useful geological tool for discriminating zones of consistent lithology and contacts between contrasting lithological units (Duval, 1983). Accordingly, four composite images were generated as follow:

1. Radioelement composite image map (K, eU and eTh).
2. Equivalent uranium composite image map (eU, eU/eTh and eU/K).
3. Equivalent thorium composite image map (eTh, eTh/eU and eTh/K).
4. Potassium composite image map (K, K/eTh and K/eU).

1. Radioelements composite image :

Different rock types have different characteristic concentrations of radioactive-elements, potassium,

uranium and thorium. Therefore, the concentrations calculated from gamma-ray spectrometric data can be used to identify zones of consistent lithology and contacts between constraining lithological units.

The three radioactive-elements composite image map (Fig. 10) of the study area shows the variations occurring in the three radioactive-elements concentrations, eU (ppm), eTh (ppm) and K (%) which mainly reflect lithological variations. The color index at each corner of the triangular legend (K in red, eU in blue and eTh in green) indicates 100% concentration of the indicated radioactive-elements. The colors at each point inside the triangle represent different ratios of the radioactive-elements, according to the color differences on the absolute three radioelements composite image map. The eU, eTh and K images emphasize the radioelement and high light areas, where the particular radioelement has relatively higher concentrations. The observed radioelement zones show a fairly close spatial correlation with the geologically mapped lithological units.

2. Uranium Composite Image:

The uranium composite image also reflects lithological differences and could be useful in geologic mapping problems (Duval, 1983). The relative concentration of uranium with respect to both potassium and thorium is an important diagnostic factor in the recognition of the possible uranium deposits (IAEA, 1988). So, the uranium composite image (Fig. 11) is generated to combines eU (in red) with the ratios eU/K (in blue) and eU/eTh (in green).

3. Thorium Composite Image:

The thorium composite image (Fig. 12) combines eTh (in red), eTh/eU (in green) and eTh/K (in blue). This image emphasizes the relative distribution of thorium and highlights areas of its enrichment. The bright color on such image is a good pointer to rock units having thorium enrichment relative to the potassium and uranium.

4. Potassium Composite Image:

The potassium composite image map (Fig. 13) combines K (in red) with K/eU (in blue) and K/eTh (in green). This image shows the overall spatial distribution of the relative potassium concentration which can be distinguished on the map as anomalous bright zones. Such areas are related to granites and wadi sediments, while dark areas are associated with areas of low K concentrations of the Tarawan and Duwi formations.

2. Factor Analysis:

The factor analysis technique has been applied to airborne gamma-ray spectrometry (Duval 1976, Wecksung 1982, Mostafa 1988 and Mostafa et al. 1990). It is a multivariate statistical technique by which variables on a sets of geophysical data (K, eU, eTh, eU/eTh, eU/K and eTh/K) are linearly combined giving rise to new fundamental quantities (factors) which can be named and simply interpreted in the light of sound geologic reasoning. The resultant factor scores are subjected to clustering after being rotated using the Varimax method. One of the major goals of the factor analysis is to reduce the complexity of data matrices (Klovan 1968) where, the number of variables reduces to the minimum number of independent variables which adequately described the data.

Factor analysis computation involves three major steps; the correlation matrix, factor extraction and factor rotation. The correlation matrix indicates to some extent that variables are related to each other. The factor extraction determines how many factors constructs are needed to account for the pattern of values found in the correlation matrix. This process involves a numerical procedure that uses the coefficients in the (R) matrix to produce factor loadings.

The correlation matrix of the spectrometric variables of the study area is calculated and presented in Table 1. Three principle factors F1, F2 and F3 are extracted from table 1 after being rotated using the varimax method (Table 2). The computed scores values of the three factors are represented as two-dimensional score contour maps for F1, F2 and F3 as in (Figs. 14, 15 and 16) respectively. The first factor (F1) can be recalled as a factor of integrated radioactivity. The second factor (F2) and the third factor (F3) are recalled as factors of differentiating rock types.

In order to display the overall spatial distribution of the radioelement differences in the study area, the factor scores characterizing the different rock units in the three factors F1, F2 and F3 are combines as F1 (in red) with F2 (in green) and F3 (in blue) to generate the factor scores composite image map (Fig. 17).

3. Statistical Treatment of the Ground Spectrometric Data

The collected spectrometric data (TC, eU, eTh and K) are in the form of digital grids, from which three ratios (eU/eTh, eU/K and eTh/K) were calculated. A composite file was prepared to include seven columns (TC, eU, eTh, K, eU/eTh, eU/k and eTh/K) and rows of sample points. Standard statistics were applied to the raw data to compute mean, minima, maxima, standard deviation and normality check for each variable (Table 3).

The statistical treatment of the ground gamma-ray spectrometric data depends mainly on the application of the coefficient of variability (CV). For a certain variable value in the study area, if the (CV %) is less than 100% (Koch et al 1972) in Sarma and Koch 1980, the variables tend to exhibit normal distribution according to the following relation:

$$CV\ \% = (\sigma/X) \times 100$$

where: σ is the standard deviation, X is the arithmetic mean.

Table (3) presents the results of the statistical treatment which was applied on the seven variables (TC, eU, eTh, K, eU/eTh, eU/K and eTh/K) in the whole study area. Table (4), summarize the statistical results of the seven variables of the five interpreted lithoradiometric units.

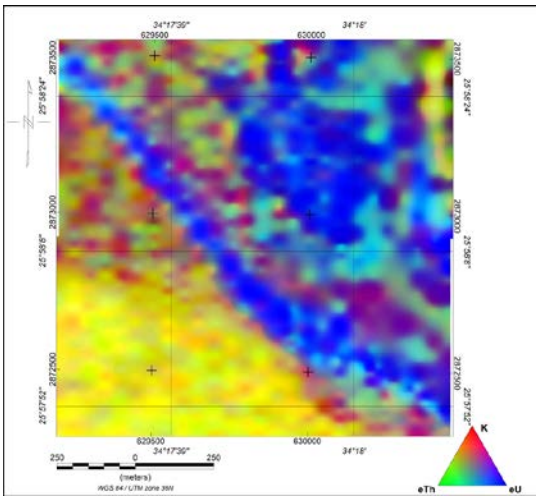

Fig. (10): False color absolute radioelements (K, eTh, and eU) composite image map.

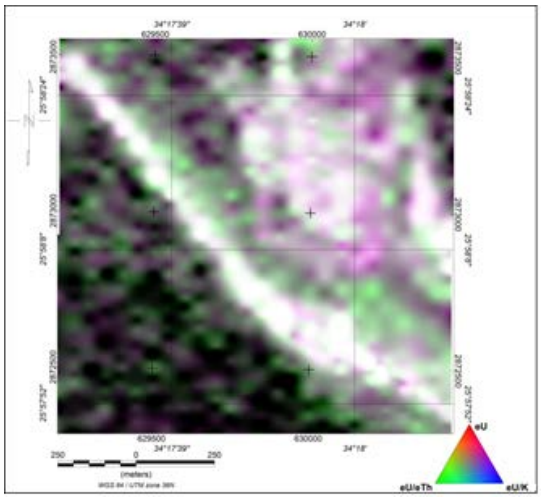

Fig. (11): False color uranium composite image map.

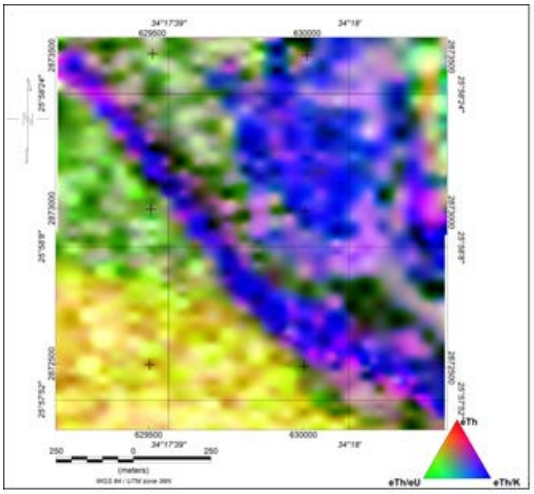

Fig. (12): False color thorium composite image map.

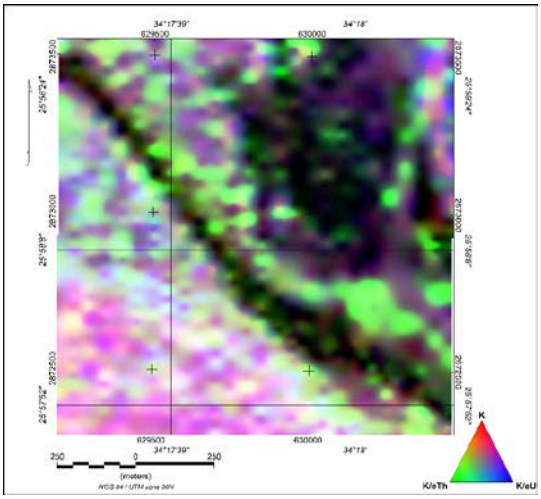

Fig. (13): False color potassium composite image map.

Table (1): Correlation coefficient between the seven data variables.

Variables	TC (Ur)	K (%)	eU (ppm)	eTh (ppm)	eU/eTh	eU/K	eTh/K
TC (Ur)	1.00						
K (%)	0.33	1.00					
eU (ppm)	0.62	-0.51	1.00				
eTh (ppm)	0.38	0.75	-0.33	1.00			
eU/eTh	0.37	-0.44	0.74	-0.45	1.00		
eU/K	0.46	-0.43	0.77	-0.26	0.60	1.00	
eTh/K	0.12	-0.53	0.50	-0.09	0.21	0.72	1.00

Table (2): Varimax factor loadings matrix for the seven variables.

	Component		
Variables	**1**	**2**	**3**
TC (Ur)	0.79	0.58	0.09
K (%)	-0.12	0.83	-0.46
eU (ppm)	0.85	-0.20	0.41
eTh (ppm)	-0.17	0.94	0.02
eU / eTh	0.84	-0.40	0.04
eU /K	0.63	-0.13	0.68
eTh /K	0.12	-0.09	0.98

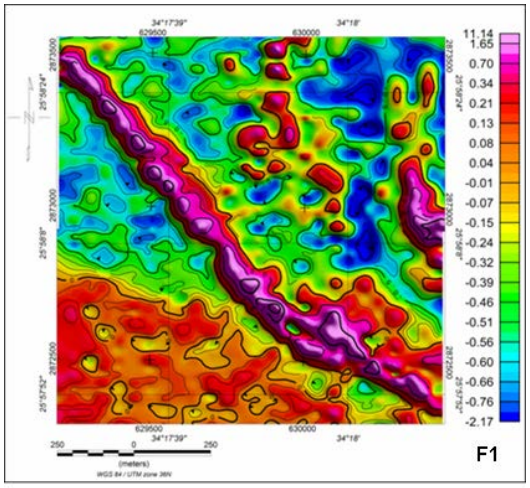

Fig. (14): Filled color contour map of the first factor (F1) map.

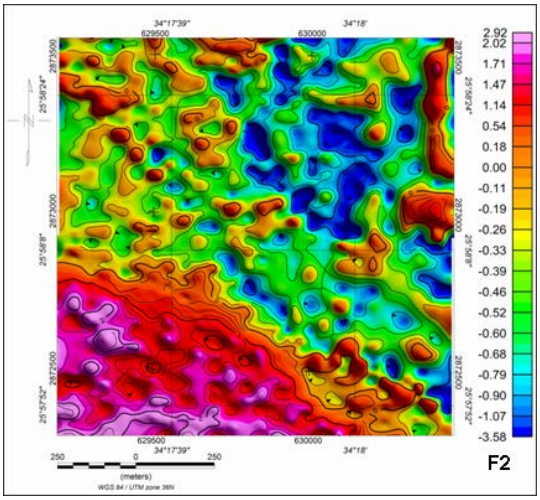

Fig. (15): Filled color contour map of the second factor (F2)map.

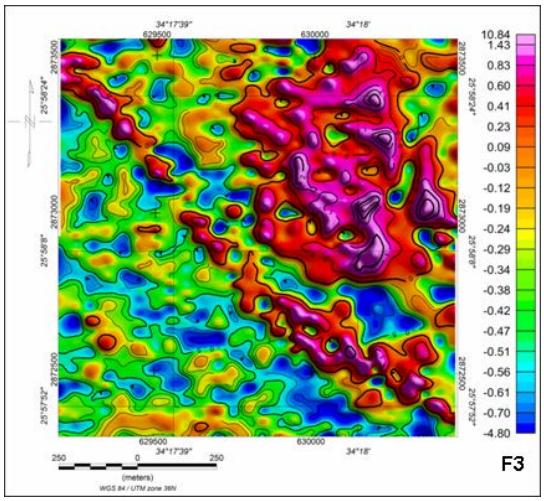

Fig. (16): Filled color contour map of the third factor (F3) map.

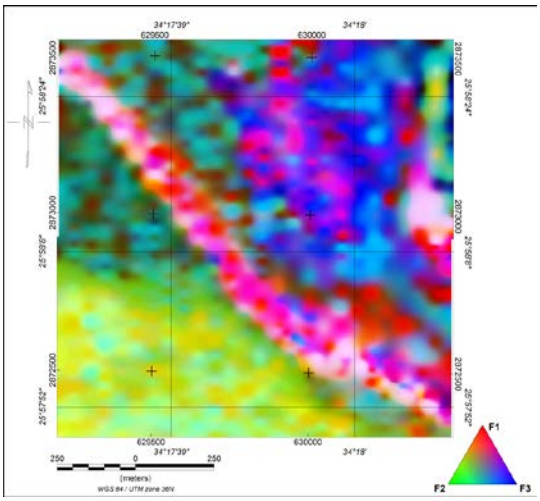

Fig. (17): False color composite map of F1, F2 and F3 factor scores.

Table (3): Statistical analysis of the radioelements in the study area.

Variables	Min.	Max.	Mean (X)	Standard Deviation (σ)	Coefficient of Variability (CV %)
TC (Ur)	4.1	52.6	14.3	5.8	40.1
K (%)	0.1	4.2	1.7	1.1	68.5
eU (ppm)	0.1	51.0	5.9	6.2	102.9
eTh (ppm)	0.3	14.0	4.7	2.3	50.0
eU/eTh	0.02	7.6	2.1	3.6	171.7
eU/K	0.06	48.0	11.9	28.1	236.3
eTh/K	0.42	11.60	4.3	4.0	93.4

Table (4): Statistical analysis of the radioelements in the interpreted lithoradiometric units.

I. L.R.U.	No.	Variables	Min.	Max.	X	σ	CV %	X+1σ	X+2σ	X+3σ
WS	389	TC	8.1	18.8	11.3	13.0	12.7	24.3	37.3	50.3
		K	0.2	3.4	1.7	0.5	28.2	2.1	2.6	3.07
		eU	0.5	9.7	3.1	1.7	53.8	4.8	6.5	8.2
		eTh	1.1	7.9	4.4	1.3	29.2	5.7	6.9	8.2
		eU/eTh	0.1	4.3	0.8	0.6	70.6	1.4	1.9	2.5
		eU/K	0.2	39.5	2.7	4.0	148.0	6.6	10.5	14.5
		eTh/K	0.7	26.3	3.1	2.7	87.1	5.9	8.6	11.3
DU	268	TC	6.0	52.6	18.2	8.2	45.0	26.4	34.6	42.8
		K	0.1	2.2	0.8	0.5	63.2	1.2	1.7	2.2
		eU	2.3	51.0	13.9	8.7	31.2	22.5	31.2	39.9
		eTh	0.3	8.2	3.1	1.5	50.1	4.6	6.1	7.6
		eU/eTh	0.5	67.3	5.9	6.1	102.5	12.0	18.0	24.1
		eU/K	1.3	379	36.1	50.8	141.0	68.9	137.0	188.0
		eTh/K	0.4	44.0	6.0	5.8	96.7	11.8	17.7	23.5
GR	256	TC	10.7	28.0	19.2	1.8	9.2	20.9	22.7	24.5
		K	1.7	4.2	3.4	0.4	11.1	3.8	4.2	4.5
		eU	0.2	6.4	2.5	1.0	36.1	3.7	4.7	5.7
		eTh	2.2	14	7.9	1.9	23.8	9.8	11.6	13.5
		eU/eTh	0.1	1.5	0.4	0.2	57.9	0.6	0.8	1.1
		eU/K	0.1	2.9	0.8	0.4	42.8	1.2	1.5	1.9
		eTh/K	0.6	4.3	2.3	0.5	23.4	2.9	3.4	3.9
TA	200	TC	4.4	15	9.7	1.6	16.7	11.3	12.9	14.6
		K	0.2	2.1	0.6	0.4	59.3	0.9	1.3	1.6
		eU	2.0	11.6	6.1	2.0	33.1	8.1	10.1	12.2
		eTh	1.0	8.0	3.3	1.3	38.6	4.6	5.9	7.2
		eU/eTh	0.4	9.1	2.2	1.3	59.1	3.5	4.8	6.1
		eU/K	1.3	58.0	15.6	12.0	77.0	27.6	39.6	51.6
		eTh/K	1.3	24.0	7.0	3.8	54.0	10.8	14.6	18.4
MG	20	TC	4.1	13.5	7.6	2.6	34.9	10.2	12.8	15.4
		K	0.7	2.0	1.2	0.4	31.1	1.6	1.9	2.3
		eU	0.1	3.6	1.6	1.0	60.5	2.6	3.6	4.6
		eTh	1.8	8.0	3.8	1.6	42.8	5.4	7.1	8.7
		eU/eTh	0.1	1.3	0.5	0.3	69.1	0.8	1.2	1.5
		eU/K	0.1	2.7	1.3	0.7	51.8	2.0	2.7	3.4
		eTh/K	1.4	6.0	3.3	1.4	41.4	4.7	6.1	7.4

Explanation:

No. = Number of observations, I.L.R.U. = Interpreted lithoradiometric unit, X =Arithmetic mean, σ = Standard deviation, CV% = Coefficient of variability, Min. = Minimum value, Max. = Maximum value, WD = wadi deposits, DU = Duwi formation, GR = Granite rocks, TR = Tarawan formation, MG = Meta-Gabbro, TC in Ur, eU in ppm, eTh in ppm and K in %.

RESULTS AND DISCUSSION

Examination of the ground gamma-ray spectrometric maps reveals the existence of a wide range of radiometric levels variations, indicating to surficial rocks of various compositions. It is evident from the correlation between the different rock units and their recorded radiometric levels that, on a regional scale, the pattern of ground radioactivity is closely connected with the surface geology of the area. The collected field data were qualitatively and quantitatively interpreted in order to distinguish between various lithologic units from the point of view of radioelement concentrations and delineating the surface contacts between these interpreted radiometric-lithologic units.

Qualitative Interpretation:

The qualitative interpretation of ground spectrometric survey data depends mainly upon the correlation between the general pattern and surface distribution of the spectrometric measurements and the various types of lithological units recorded in the geological map (Fig. 2). Careful examination of the ground spectrometric maps (Figs. 3 to 9) indicate three levels displayed with filled colored contours. The total count map (Fig. 3) shows radiometric values varies between 4.1 and 52.6 Ur. The low radiometric zone attains values less than 10 Ur, and the moderate one is ranging between 10 to 14 Ur, while that of high values exceed 14 Ur is observed mainly as a linear anomalous zone over the Duwi Formation on the NW phosphatic ridge, and younger granites at the northeastern and southwestern portions of the study area.

The eU values reach to 51 ppm (Fig. 4), where the values less than 2.5 ppm associated with the wadi deposits represent the lower concentrations. The second level (from 2.5 to 5 ppm) is recorded over the granitic rocks and their debris on the southwestern parts of the study area. The third level possesses relatively high concentrations up to 51 ppm eU related mainly to the Tarawan Formation as well as the phosphate of the Duwi Formation on the NW ridge.

Among three observed levels of the equivalent thorium contour map (Fig. 5), the lowest one with values from 1 to 3 ppm associated with the Duwi and Tarawan formations. The second intermediate level (from 3 to 4.5 ppm) corresponds to wadi sediments and the third level of eTh up to 14 ppm is mainly related to the granitic rocks at the northeastern and southwestern parts in the area.

Similar to the other radioelement maps, the potassium contour map (Fig. 6) shows three levels. The lowest level (less than 1%) is clear to map the linear feature of the NW Duwi phosphatic ridge and the Tarawan Formation. The values ranging from 1 to 1.6 % of K represent the intermediate level on the wadi deposits. The highest K values constituting the third level from 1.6 to 4.2 % are mainly associated with the granitic rocks and their debris in the southwestern parts and small portion in the northeastern part.

The equivalent uranium/equivalent thorium (eU/eTh) contour map (Fig. 7) is close to the eU (Fig. 4) map with great similarity. The lowest values recorded in the map are related to granite rocks in the southwestern and northeastern part of the area. Meanwhile, the highest values are recorded over the Duwi Formation on the NW ridge and on the Tarawan Formation. The eU/K map (Fig. 8) resembles the eU/eTh map (Fig. 7) since the high anomalies reflect concentration of eU and absence of eTh and K%. The high anomalies are located over the Duwi Formation in the phosphatic ridge and Tarawan Formation. The rest of the area possesses generally low eU/K values, especially at the southwestern part associated with the granitic rocks exposures see. The eTh/K contour map (Fig. 9) shows a degree of similarity to eU/eTh map (Fig. 7) and eU/K map (Fig. 8). This similarity may be due to the poorness of K% relative to the two other elements (eU and eTh). The higher values are observed over the Duwi and Tarawan formations. Meanwhile, the lowest values are observed generally over the granitic rocks and wadi deposits.

Relationship between Radioactivity and Surface Geology:

The relationship between ground radioactivity measurements and geology has been interpreted according to the radiometric levels inferred from the different geologic and radiometric maps Figs. (2-9). It is evident from the correlation between the different rock units and the recorded radiometric levels on a regional scale, the pattern of radioactivity is relatively reflects the surface geology of the area under study. The areas of low radiometric levels coincide mainly with the wadi deposits while those with moderate levels are observed over the Tarawan Formation and the high levels are associated with the Duwi Formation and younger granites.

The phosphates of the Duwi Formation have special importance where they possess the highest radioactivity values among the different rock units in the area. The zone of phosphatic exposure in the area trends approximately to the NW direction in a linear pattern. From the radioactivity point of view, the investigated radiometric maps revealed that the phosphates of the Duwi Formation are easily recognized and delineated with sharp contacts with the adjacent rock units. The observed disruption of the radioactive contours and the difference in amplitudes of their associated closed anomalies in this phosphatic zone may be attributed to assumed faults.

From the three radioactive-elements composite image map (Fig. 10) it was noticed that, the higher blue zone reflects higher concentrations of the eU rather than the eTh and K. This zone coincides with the phosphates of the Duwi Formation and the Tarawan Formation. The red spots in the map refer to K concentrations which are correlated with the wadi sediments. The map indicates that the area is relatively poor in eTh which is restricted in the northeastern portion of the area related to

granites. The yellow color distinguishes broad zones in the map where there is equality in the concentration of the eTh and K in these zones which are associated with granitic rocks and wadi sediments. The radioelement composite image shows excellent similarity with the geological map of the study area.

Since the area is relatively poor in eTh and K, the uranium composite image map (Fig. 11) indicates clear bright areas of enriched uranium concentration forming three zones correlated with linear anomalies of the phosphates of the Duwi and Tarawan formations in the central northern parts of the area. In spite of the absence of bright color from the thorium composite image map (Fig. 12), as indicative to the poorness of thorium, the blue and green colors prove increasing the thorium concentrations relative to potassium in the study area. The potassium composite image map (Fig. 13) shows black areas of low K concentrations within the Tarawan and Duwi formations, while the bright areas are related to the granites and wadi sediments.

Quantitative Interpretation:

The quantitative interpretation depends principally upon the fact that, the absolute and relative concentrations of the radioelements (K, eU and eTh) vary measurably and significantly with lithology (Darnley and Ford, 1989). The quantitative treatment of the spectrometric data in the present study is discussed on the light of the factor analysis technique and the statistical treatment. Statistical computation was applied to the original spectrometric data without applying any transformation, in accordance with the recommendation given by Sarma and Koch (1980).

The correlation matrix (Table 1) shows that the total count (T C) is highly correlated positively with eU (62.3 %) and weakly correlated with eTh, K, eU/eTh, eU/K, eTh/K as 37.5, 32.6, 37.4, 45.5 and 12% respectively. The equivalent uranium (eU) is highly correlated with their ratios; eU/eTh and eU/K as 74 and 77 % and moderately correlated with eTh/K with 50 %. It is observed that eU is reversely correlated with the K and eTh where they recorded -51 and -33 % respectively. The eU/K is positively correlated with eU/eTh where the ratio reaches to 66 %. Table 2 shows the three principle factors; F1, F2 and F3 that extracted from table 1, after their rotation by using the Varimax method. It can be noticed form this table that, factor one (F1) has an appreciably high positive loading with the four variables TC, eU, eU/eTh and eU/K as 79, 85, 84 and 63 % respectively. F1 (Fig. 14) exhibits inverse weak loading with the eTh and K as -17 and -12 %. Therefore, F1 can be identified as the factor of integrated radioactivity or the factor of uranium exploration (Mostafa et al, 1990). The second factor (F2) is positively highly loaded with K and eTh as 83 and 93 % respectively and moderately positive loaded with TC with 57 %. F2 (Fig. 15) is inversely loaded with the eU, eU/eTh, eU/K and eTh/K as -20, -40, -13 and -9 % respectively. The third factor (F3) is positively high loaded factor with the eU/K and eTh/K by 68 and 98 % respectively (Fig. 16), while, it has weak to very weak positive loadings with the TC, eU, eTh, and eU/eTh by 9, 41, 0.9 and 4 % respectively and inversely loaded with K as 46 %.

The results obtained from the application of the factor analysis technique, made it possible to delineate new geologic units and correct some rock types on the geologic map of the study area through merging the three factor scores as composite ternary image map (Fig. 17). It was found that this map shows a relative similarity to the geologic map of the study area. The matching between the factor scores maps and the resultant composite image map enables to generate an interpreted lithoradiometric unit map (Fig. 18). It could be easily to recognize five lithoradiometric units in the map with high degree of correlation with those found in the geologic map (Fig. 2).

Identification and Outlining the Uraniferous Provinces:

According to Saunders and Potts (1976), defining the broad uraniferous provinces (in which the rocks and soils are rich in U) is one of the important spectrometric data interpretation steps. Most of the world's important U deposits are clustered in few areas or provinces which appear to persist through long periods of geologic time, with the U being moved from one type of deposit to another within each province by normal erosional, sedimentary and igneous processes. Such provinces are characterized by U-rich rocks and the presence of a variety of U types. These and other similar observations led to the conclusion that new U deposits will be found more frequently in regions geochemically rich in U than those where the U content is low (Klepper and Wyant, 1957). The occurrence of U mineralization seldom occurs in isolation, and they are normally found in association with both regional and local zones of enrichment which is amenable to detection. The relative concentrations of U with respect to both Th and K are an important diagnostic factor in the recognition of the possible U deposits from gamma-ray spectrometric data (IAEA, 1979). Moreover, the most important parameters which can be measured are the relative concentration of U to Th and U to K taken in conjunction with the U measurements. They are diagnostic for the identification of zones of anomalous U concentration (Darnley, 1973).

In the present work, it is important to statistically examine the spectrometric data to identify and outline a significant eU anomaly on the basis of exceeding two and three standard deviation levels above the mean for single points, which show local enrichment of eU over eTh and K % in terms of statistically high eU/eTh and eU/K values. This type of statistical treatment of data provides a mean of searching for areas showing high uranium anomaly content within each unit. Results of such statistical treatment are given in table 4. The local point anomaly map (Fig. 19) shows the location and magnitude of deviation from the mean for eU, eTh, eU/eTh and eU/K.

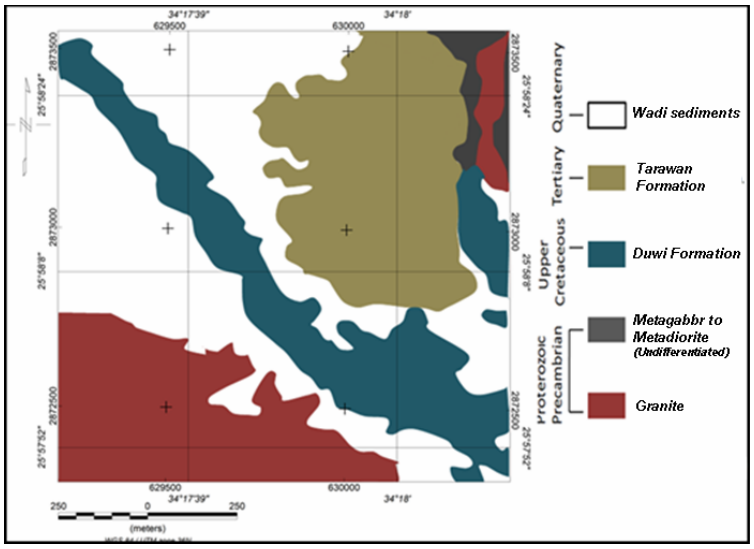

Fig. (18): Interpreted lithoradiometric units map (ILRU).

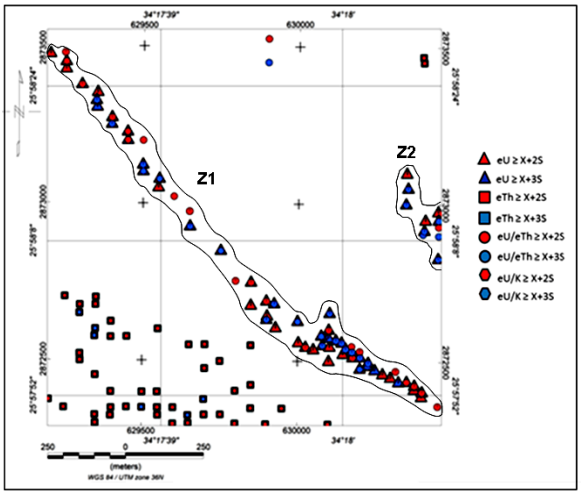

Fig. (19): Point anomaly map of the area.

It also shows the anomalies that their values exceed (X + 2S) and (X + 3S). It is observed from the map that there are two zones of uranium anomalies proving radioactive mineralization in the area under consideration. These zones denoted as (Z1 and Z2) possess high eU, eU/eTh and eU/K values of X+2S and X+3S and are observed over the Duwi Formation of Phosphatic composition. Nevertheless, there are another radiometric anomalies are attributed to the eTh which have values exceeding than X+2S and X+3S related generally to the granitic rocks. It is clear from the point anomaly map that the radioelements correlated to phosphatic zone and could be structurally controlled.

CONCLUSION

Zog El-Bohar area is a part of the Central Eastern Desert of Egypt, about 15 km. to the Southwest of Quseir Town on the Red Sea Coast. It lies betwen latitudes 25^{o} 57′ 49.29″ N & 25^{o} 58′ 27.91″ N and longitudes 34^{o} 17′ 25.92″ E & 34^{o} 18′ 11.31″ E. It is generally covered by metagabbro and granites as Precambrian rocks as well as Phanerozoic sediments involving Duwi Formation of phosphatic composition, Tarawan Formation and Quaternary deposits.

The ground gamma-ray spectrometric data have been conducted, analyzed and interpreted qualitatively and quantitatively in order to identify the uraniferous anomalous zones in the area. So, the radioelements (K %, eU in ppm and eTh in ppm) contour maps as well as ratio maps (eU/eTh, eU/K and eTh/K) were prepared. It is evident from the correlation between the different rock units and the measured levels of gamma radiation over them that, on a regional scale, the pattern of the radioactivity is closely correlated with the simplified surface geology of the area.

Composite false color imaging indicated that the bright areas which reflect the higher concentrations of the radioelements are mainly correlated with the phosphates of Duwi Formation as well as some small scattered spots associated with the Tarawan Formation.

Four interpreted litho-radiometric units could be

distinguished in the area through application of factor analysis technique. A statistical treatment is carried out on the data in order to interpret it quantitatively. Defining significant radioactive anomalies was performed by calculating the upper significant factor or threshold, (X+2S) and (X + 3S), for eU, eTh, eU/eTh and eU/K measurements in each rock unit. It has been used as a quantitative technique to confirm outlining the anomalous provinces which form two zones as shown in the point anomaly map. The outlined uraniferous provinces are correlated to the uranium-bearing phosphatic Duwi Formation, as well as could be structurally controlled.

The authors highly recommended to follow up the investigation of the studied area which is considered as a very important source of petroleum (from black shales) and phosphates as well as a possible source for uranium and rare chemical elements.

REFERENCES

Abdel Razik, T.M., (1967): Stratigraphy of the sedimentary cover of Anz-Atshan, south Duwi district. Bull. Fac. Sci., Cairo univ. 41:pp153-179.

Abdel Razik, T.M., (1972): Comparative studies on the upper cretaceous - early Paleocene sediments of the Red Sea coast, Nile valley and western desert, Egypt. 8th. Arab petrol. Congr. Algiers, paper (B-3). 23p.

Ahmed, A.H. and Arai, S., (2002): Platinum-Group Element Geochemistry in Podiform Chromitites and Associated Peridotites of the Precambrian Ophiolite, Eastern Desert, Egypt. 9th International Platinum Symposium. Jul. 21-25, 2002, Montana, Billings, USA, pp. 1-4.

Akkad, S.E. and Dardir, A., (1966): Geology of the red sea coast between Ras Sharga and Mersa Alam with short note on the exploratory work at Gebel El Rusas lead-zinc deposits. Geol. Surv. Egypt, paper 35,67p.

Ball, J. (1913): A brief note on the phosphate deposits of Egypt. Egypt. Surv. Dept., 6p.

Barron, T. and Hume, W.F., (1902): Topography and geology of the eastern desert of Egypt (central portion). Egypt. Surv. Dept., 331p.

Beadnell, H.J.L., (1924): Report on the geology of the Red Sea coast between Quseir and wadi Ranga. Petrol.res.bull 13, government press, Cairo.

Conoco, (1989): Stratigraphic lexicon and explanatory notes to the geological map of Egypt 1:500 000. Conoco Inc., Cairo, Egypt, 251 p.

Darnley, A.G., (1973): Airborne gamma-ray survey techniques, present and future, in uranium exploration methods, proceeding of panel; International Atomic Energy Agency, Vienna, pp. 67-108.

Darnley, A.G.and Ford, K. L., (1989): Regional airborne gamma ray surveys a review.Proceedings of Exploration, 87; Third Decennial International Conference on Geophysical and Geochemical Exploration for Minerals and Groundwater, Edited by G. D. Garland, Ontario, Canada, Geol. Sur., of Canada, Special Vol. 3, pp. 229-240.

Duval, J.S., (1976): Statistical interpretation of airborne gamma-ray spectrometric data using factor analysis: Proceeding of a symposium on Exploration of Uranium ore deposits. Vienna, IAEA. SM. 208/12.

Duval, J.S., (1983): Composite colour images of aerial gamma-ray spectrometric data; Geophysics, Vol. 48, No. 6, pp. 722-735.

Dyni, John R. (2006): Geology and resources of some world oil shale deposits.Scientific Investigations Report 2005–5294. United States Department of the Interior,United States Geological Survey. Retrieved 2007-07-09.

El-Shazly, E.M. and Abdallah, A.M., (1964): paper no. 31, Geology of sulphur occurrence of Ranga, Eastern Desert.10 p., 5 pl.

EL-Shazly, E.M., (1977): The geology of the Egyptian region. In: A.E.M. Narin, W.H. Kanes & F.G. Stelhi (eds), the Ocean basins and margins. Plenum press 4(A): pp379-444.

Faris, M.I. and Hassan, M.Y., (1959): Report on the stratigraphy and fauna of the Upper Cretaceous rocks of Um El Hueinat, Safaga area. Bull. Fac. Sci., Ain Shams Univ. 4:191-207.

Gindy, A.R., Ghobrail, W.W., and Badra, E.E., (1973): Studies on Egyptian phosphates; I: thickness, phosphorous content, alpha radioactivity of the exploited phosphorite bed in Hamrwein area, Red Sea province, Egypt. Proc. Egypt. Acad. Sci. 26:1-17.

Gindy, A.R., Ghobrail, W.W., and Badra, E.E., (1976): Studies on Egyptian phosphates; II: intraphosphatic succession, mechanical analyses and radioactivity of the exploited bed units in Hamrawein area, Red Sea province, Egypt. Proc. Egypt. Acad. Sci. 29: 129-144.

International Atomic Energy Agency (IAEA), (1979): Gamma-ray surveys in uranium exploration, IAEA, Vienna, Austria; Technical Report Series No. 186, 90 p.

International Atomic Energy Agency (IAEA), (1988): Geochemical exploration for uranium; IAEA Technical Report Series No. 284, Vienna, Austria, 97 p.

International Atomic Energy Agency (IAEA), (2003): Guidelines for radioelement mapping using gamma ray spectrometry data; Vienna, Austria, 173p.

Issawi, B., Francis, M., El Hinnawi, M., and Mehanna, A., (1969): Contribution to the structure and phosphate deposits of Quseir area. Geol. Surv. Egypt, paper 50, 35p.

Issawi, B., Francis, M., El Hinnawi, M., and El Deftar, T., (1971): Geology of the Safaga-Quseir coastal plain and of Mohamed Rabah area. Ann. Geol. Surv. Egypt 1:1-19.

Khalil, S. M. and McClay, K.R., (2002): Extensional fault-related folding, northwestern Red Sea, Egypt, Journal of Structural Geology 24 (2002), pp. (743-762).

Klepper, M.R. and Wyant, D.G., (1957): Notes on the geology of uranium. USGS Bull., 1046-F, 87-148.

Klovan, J.E., (1968): Selection of target areas: A paper presented at the symposium on Decision-making in Exploration, Vancouver, Jan. 26. 1968, 9p.

Mostafa, M.E., (1988): Analysis of integrated geologic data for uranium exploration in Egypt. Case study, Tectonics of the fractures bearing U-mineralization in the younger granitoids, Central Eastern Desert, Egypt. International Atomic Energy Agency (IAEA), Vienna, 172-184.

Mostafa, M.E., Rabie, S.I., and El-Rakaiby, M.L., (1990): Rock unit mapping using Factor analysis applied to airborne gamma - ray spectrometric data, West G. Qattar, Egypt. Annals of Geo. Survey. Egypt, XVI (1986-1989), 295-300.

Sabet, A.H., Bessonenko, V.V., and Bykov, B.A., (1976): The intrusive complexes of the central eastern desert of Egypt. Ann. Geol. Surv. Egypt 6: pp. (53-73).

Sarma, D.D., and Koch, G.S., (1980): A statistical analysis of exploration geochemical data for uranium; Mathematical Geology, 12 (2), pp. 99-114.

Saunders, D.F., and Potts, M.J., (1976): Interpretation and application of high sensitivity airborne gamma-ray spectrometer data. IAEA Symposium on Exploration for uranium ore deposits, Vienna, Austria, IAEA-SM 208/45, pp. 107-124.

Tarabili, E.E., (1966): General outline of epeirogenesis and sedimentation in region between Safaga and Quseir and southern wadi Qena area, Eastern desert, Egypt. Bull. Am. Assoc. petrol. Geol. 50:pp1890-1898.

Tarabili, E.E., (1969): Paleography, paleoecology and genesis of the phosphate sediments in Quseir-Safaga area, UAR. Econ. Geol. 64:pp172-182.

Wecksung, G.W., (1982): A factor analysis approach for comparing aerial radiometrics with other related data sets : Geophysics, special research workshops, V. 47, No. 4, pp 408 - 409.

Youssef, M.I., (1957): Upper Creataceous rocks in kosseir area. Bull. Inst. Desert Egypte 7(2): pp35-54.